Two Methods for Calculating the Velocities Induced by a Constant Diameter Far-Wake

D. H. Wood* and C. Meyer†
University of Newcastle, Newcastle, New South Wales, 2308, Australia

This paper describes two methods for calculating the velocities induced by the constant diameter helical vortices that occur in the far-wakes of helicopter rotors in hover or vertical flight, propellers, and horizontal-axis wind turbines. The velocities involve infinite integrals which, in general, cannot be integrated analytically. In the first method, each integral is evaluated numerically up to a finite limit and the remaining integral is approximated by an analytical function. The integrand of each function, or "remainder," is found by summation over all of the vortices shed at the same radius. Numerical experiments show the remainders have a computational efficiency similar to those derived previously. The main features of the present remainders are simplicity and versatility. Furthermore, the remainders can replace numerical integration in some special cases. In the second method, the range of integration is made finite by transforming the integrand into one containing an infinite sum. The sum is approximated using the Euler-Maclaurin formula, and the resulting integral is evaluted numerically. The method is more cumbersome than the first but is robust, very accurate, and should be particularly useful at small vortex pitch.

Nomenclature

$F_2, \ldots, F_{10}$ = remainder functions defined in Eq. (12)
I_u, I_v, I_w = integrals that determine u_i, v_i, and w_i, see Eqs. (1-4)
I_{ur}, I_{vr}, I_{wr} = remainders used in Method 1, see Eq. (5)
I_u, I_v, I_w = integrands defined in Eqs. (2-4)
I_{ur}, I_{vr}, I_{wr} = integrands of remainders, see Eqs. (11) and (14)
N = number of blades
p = vortex pitch
$R, R(j,N)$ = lengths defined in Eq. (6) and Eq. (2), respectively
R_α = length defined in Eq. (15)
r = radius
u_i, v_i, w_i = x,y,z velocities (respectively) induced by the trailing helical vortices
X = $p\theta + x_v - x_i$
x,y,z = coordinate directions defined in Fig. 1
α_j = $\theta + \theta_v - \theta_i + 2\pi j/N$
α_0 = $\theta + \theta_v - \theta_i$
δ = $r_i r_v / R^2$
ϵ = absolute error in approximating I_u, I_v, I_w
Γ = trailing vortex strength divided by tip radius
θ = angle defined in Fig. 1
θ_m = upper limit for finite integrals, see Eq. (5)
θ_0 = initial interval in integration of I_u, I_v, and I_w

Subscripts

i = point at which induced velocities are required
j = blade number (not number of blades)
m = value when $\theta = \theta_m$
v = refers to trailing vortex

Introduction

MODERN computational models for helicopters in hover or vertical flight, propellers, and horizontal-axis wind turbines share many features. Of interest here is the far-wake that, in each case, can be assumed to contain a number of helical vortices of constant pitch and diameter, e.g., Langrebe,[1] Kerwin,[2] Hess and Valerazo,[3] and Valerazo and Liebeck.[4] Any such vortex is part of a symmetrical system of vortices trailing from the N blades spaced $2\pi/N$ radians apart. They influence the flow over the blades through the Biot-Savart law that gives the three induced velocities in terms of infinite integrals. Unfortunately, these integrals have no general analytic solution, and so their evaluation requires some form of approximation. Perhaps the simplest approximation is to replace the helices by a number of short, straight vortex segments whose induced velocities are easily calculated, e.g., Afjeh and Keith[5] and Kerwin.[2] Chiu and Peters[6] criticized this method on the grounds of numerical accuracy. However, the accuracy is probably comparable to that usually achieved in modeling the blades; for example, the classical panel methods of Smith and Hess[7] and Hess[8] use flat rectangular panels to represent curved blade surfaces. The main problem would seem to be in deciding how far downstream to continue the vortex segments. Other methods that replace the helices by analytically tractable vortices include those of Miller[9] and Hess and Valerazo.[3] These methods involve either special functions or algebraic approximations to special functions.

Alternatively, the integrals can be treated directly, by the approach pioneered by Rand and Rosen[10] and developed further by Graber and Rosen[11] and Chiu and Peters.[6] Each integral is evaluated numerically up to a finite limit, and to this is added an analytic "remainder" approximating the integral over the remaining infinite range. In Refs. 6, 10, and 11, the remainder is the sum over all blades of a mean of the upper and lower bounds to the integral for each blade. The remainders are very efficient computationally; for example, their use can reduce by two orders of magnitude the amount of numerical integration necessary to achieve a reasonable accuracy.[6] Wood and Gordon[12] obtained alternative remainders by summing over the N blades before integrating. Their remainders are considerably simpler than those in Ref. 6 but are not as efficient computationally, especially at small values of vortex pitch.

This paper describes two methods for the calculation of the induced velocities. The first (Method 1) is a generalization of, and an improvement on, the method of Wood and Gordon[12] for $N \geq 2$. Their remainders are the leading terms in the series derived here. For small values of vortex pitch, the additional terms in the series result in a computational efficiency com-

Received Jan. 8, 1990; revision received July 20, 1990; accepted for publication Aug. 26, 1990.

*Senior Lecturer, Department of Mechanical Engineering.
†Visiting Student from University of Karlsruhe, Germany.

parable to that obtained by Chiu and Peters.[6] The first major feature of the new remainders is the ability to alter the number of terms in the series to obtain a desired accuracy. Second, but perhaps less important, they become simpler as N increases, whereas the computation time needed for the remainders of Refs. 6, 10, and 11 is proportional to N. It is also possible that the remainders can replace numerical integration in some special cases that are noted later. However, as pointed out by a reviewer, the existence of these special cases is not likely to reduce significantly the amount of numerical integration required for the analysis of a real blade or rotor.

The second new method (Method 2) is based on rewriting the infinite integral for each vortex as an integral containing one or more infinite series. These series are summed exactly up to a finite limit, and the remaining infinite sums are approximated using the well-known Euler-Maclaurin summation formula. The finite integrals are evaluated numerically. The procedure seems particularly suited to small vortex pitch, where the analytic remainders are least efficient.

Method 1 is described in the next section. This is followed by a discussion of its use, based mainly on the test case used by Chiu and Peters.[6] Method 2 is then described. The subsequent section contains a general discussion of the two methods and the final section has a summary and conclusions. All of the programs used here for $N=2$ can be obtained at no cost by writing to the first author.

Method 1: Analytic Remainders

The axial velocity induced by the vortices at radius r_v, trailing from the N blades is given by

$$u_i = \frac{\Gamma}{4\pi} I_u(N) = \frac{\Gamma}{4\pi} \int_0^\infty I_u(N)\,\mathrm{d}\theta \tag{1}$$

where

$$I_u(N) = \sum I_u(j,N) = r_v \sum \frac{r_v - r_i \cos\alpha_j}{R^3(j,N)} \tag{2}$$

and

$$R^2(j,N) = r_i^2 + r_v^2 - 2r_i r_v \cos\alpha_j + X^2$$

Throughout this paper, all lengths are normalized by the tip radius and an unspecified summation is over $j=0$ to $N-1$, where j is the blade number. Most of the symbols used in Eqs. (1) and (2) are defined in Fig. 1, which shows a typical paneling of a blade for a boundary integral analysis and part of one trailing vortex. In this model, trailing vortices form at all panel junctions at the trailing edge. They then either expand or contract in the near-wake—close to the blades—before reaching the far-wake where r_v and p are constant. The far-wake "begins" at a streamwise location of x_v, which is included in the definition of X. It is emphasized that Eq. (2) and Eqs. (3) and (4) are valid only for the far-wake; the corresponding equations for the near-wake are considerably more complex. Similarly, the remainders that we now derive are valid only for the far-wake.

The other induced velocities, v_i and w_i, are obtained from Eq. (1) by replacing $I_u(N)$ by $I_v(N)$ and $I_w(N)$, respectively, where

$$I_v(N) = \sum \frac{pz_i - pr_v \cos(\alpha_j + \theta_i) - Xr_v \sin(\alpha_j + \theta_i)}{R^3(j,N)} \tag{3}$$

and

$$I_w(N) = \sum \frac{-py_i + pr_v \sin(\alpha_j + \theta_i) - Xr_v \cos(\alpha_j + \theta_i)}{R^3(j,N)} \tag{4}$$

The basis of Method 1 is the rewriting of Eq. (1) as

$$I_u(N) \approx \int_0^{\theta_m} I_u(N)\,\mathrm{d}\theta + I_{ur}(N) \tag{5}$$

where the integral, with some upper limit θ_m, is evaluated numerically and $I_{ur}(N)$ is the analytic remainder approximating the integral over the range $\theta_m \le \theta \le \infty$. The obvious aim in deriving $I_{ur}(N)$ is to maximize the computational efficiency by minimizing the θ_m necessary to achieve a specified accuracy. One way to obtain an equation for $I_{ur}(N)$ is to expand $R^{-3}(j,N)$, using

$$R^2(j,N) = R^2[1 - 2\delta \cos\alpha_j] \tag{6}$$

where $R^2 = r_i^2 + r_v^2 + X^2$ and $\delta = r_i r_v / R^2$. Thus, $R^{-3}(j,N)$ can be expressed as

$$R^{-3}(j,N) = R^{-3}\left[1 + \sum_{k=1}^{\infty} b_k \cos^k\alpha_j\right] \tag{7}$$

where $b_1 = 3\delta$, $b_2 = (15/2)\delta^2$, $b_3 = (35/2)\delta^3$, and $b_4 = (315/8)\delta^4$, etc., and, crucially, R^{-3} is independent of j. This expansion of $R^{-3}(j,N)$ is not unique: another is given in Eq. (17) in developing the second method, and Andersen and Andersen[13] use an expansion containing integrated Bessel functions. Equation (7), however, leads to simple analytic remainders, whereas the other expansions do not. Thus, I_u for each blade can be written as an infinite series:

$$I_u(j,N) = \left[a_0 + (a_1 + a_0 b_1)\cos\alpha_j + (a_0 b_2 + a_1 b_1)\cos^2\alpha_j + (a_0 b_3 + a_1 b_2)\cos^3\alpha_j + (a_0 b_4 + a_1 b_4)\cos^4\alpha_j + \cdots\right] R^{-3} \tag{8}$$

where $a_0 = r_v^2$ and $a_1 = -r_i r_v$. An analytical integration of Eq. (8) is precluded by the cosine or α terms. They are all of the form $\cos^n\alpha_j$, where n is an integer, so that each can be equated to a sum of terms of the form $\cos k\alpha_j$, where k is also an integer. Many of these terms cancel when the integrands are summed over the N blades before integrating, because Eq. (1.341.3) of Gradshteyn and Rhysik[14] requires

$$\begin{aligned} \sum \cos k\alpha_j &= 0 \qquad \text{if } k \text{ is not a multiple of } N \\ &= N \cos k\alpha_0 \qquad \text{if } k \text{ is a multiple of } N \end{aligned} \tag{9}$$

where $\alpha_0 = \theta + \theta_v - \theta_i$. Equation (9) removes, for example, the leading α term whenever $N \ge 2$, and all of the odd-power terms when N is even. The even-power terms are treated as in the following:

$$\begin{aligned} \sum \cos^4\alpha_j &= \left[3N + 4\sum \cos 2\alpha_j + \sum \cos 4\alpha_j\right]/8 \\ &= \left[3 + 4\cos 2\alpha_0 + \cos 4\alpha_0\right]/4 \qquad \text{for } N = 2 \\ &= 9/8 \qquad \text{for } N = 3 \\ &= \left[3 + \cos 4\alpha_0\right]/2 \qquad \text{for } N = 4 \end{aligned} \tag{10}$$

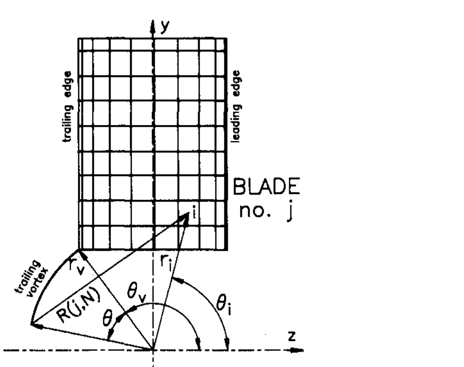

Fig. 1 Coordinate system for wind turbine. View is downstream at blade; the axial or x direction is into page. Typical distribution of panels on lower surface is shown. Blade is rotating clockwise.

where the result for $N=3$ is included for generality. As suggested by Eq. (10), the form of the remainders generally simplifies as N increases. Using the result for $N=2$, and others like it, the terms appearing explicitly in Eq. (8) can be summed to give the integrand for the remainder

$$I_{ur}(2)=\left\{\left[2r_v^2-3r_ir_v\delta+\frac{15}{2}r_v^2\delta^2-\frac{105}{8}r_ir_v\delta^3+\frac{945}{32}r_v^2\delta^4\right]\right.$$
$$-\left[3r_ir_v\delta-\frac{15}{2}r_v^2\delta^2\right]\cos 2\alpha_0-\left[\frac{105}{8}r_ir_v\delta^3-\frac{945}{32}r_v^2\delta^4\right]$$
$$\left.\times\left[\cos 2\alpha_0+\frac{1}{4}\cos 4\alpha_0\right]\right\}R^{-3} \tag{11}$$

Thus, $I_{ur}(2)$ is a finite approximation to the infinite series representation of $I_u(2)$. Equation (11) gives the highest order approximation that is considered here, but it is obviously possible to extend Eq. (11) to any arbitrary order. The remainder, $I_{ur}(2)$, is the integral from θ_m to infinity of Eq. (11). The integration involves further approximations, restricted this time to the treatment of the α terms.

Using the substitution recommended on p. 81 of Ref. 14, the integrals of the algebraic terms are of the form

$$pF_{k-1}=\int_{X_m}^{\infty}R^{-k/2}\,\mathrm{d}X=(r_i^2+r_v^2)^{(1-k)/2}\int_{X_m/R_m}^{1}(1-t^2)^{(k-3)/2}\,\mathrm{d}t$$

since $\mathrm{d}X=p\,\mathrm{d}\theta$. For the values of the integer k necessary for Eq. (11),

$$F_2=x_1/(r_i^2+r_v^2)$$
$$F_4=(x_1-x_3)/(r_i^2+r_v^2)^2$$
$$F_6=(x_1-2x_3+x_5)/(r_i^2+r_v^2)^3$$
$$F_8=(x_1-3x_3+3x_5-x_7)/(r_i^2+r_v^2)^4$$
$$F_{10}=(x_1-4x_3+6x_5-4x_7+x_9)/(r_i^2+r_v^2)^5 \tag{12}$$

where for any odd integer n, $nx_n=1-(X_m/R_m)^n$. Integration of each α term by parts leads to an infinite series in powers of p. Since the algebraic terms give a contribution to $I_{ur}(2)$ that is proportional to p^{-1}, and experience shows that only the low-order α terms are important, the series is truncated at p^1. Thus,

$$I_{ur}(2)=\frac{r_v^2}{p}\left[2F_2-3r_i^2F_4+\frac{15}{2}r_i^2r_v^2F_6-\frac{105}{8}r_i^4r_v^2F_8\right.$$
$$+\left.\frac{945}{32}r_i^4r_v^4F_{10}\right]+\frac{3r_i^2r_v^2}{2R_m^5}\left[\left(1-\frac{5r_v^2}{2R_m^2}\right)\sin 2\alpha_{0m}\right.$$
$$\left.-\frac{5pX_m}{2R_m^2}\left(1-\frac{7r_v^2}{2R_m^2}\right)\cos 2\alpha_{0m}\right] \tag{13}$$

Equation (13) can, of course, be extended to any arbitrary order, but that shown is the highest considered here. The F_2, or zeroth-order term, is the only one given by Wood and Gordon,[12] who ignored the series in Eq. (7). The importance of this term follows from

$$I_u(N)=Nr_v^2F_2(\theta_m=0)/p \qquad \text{if} \quad r_i=0$$

which can be obtained readily from Eq. (1). Thus, F_2 is the dominant term if $r_i \ll r_v$, whereas F_2 and F_4 terms dominate if $r_v \ll r_i$. These are the special cases where the remainders can possibly replace numerical integration.

Because Eq. (9) remains valid if the cosine terms are replaced by sine terms [see Eq. (1.341.1) of Ref. 14], a similar analysis is possible for $I_{wr}(2)$. To the same order as in Eq. (11), this gives

$$I_{wr}(2)=y_i\left[-2F_2+3r_v^2F_4-\frac{15}{2}r_i^2r_v^2F_6+\frac{105}{8}r_i^2r_v^4F_8\right.$$
$$\left.-\frac{945}{32}r_i^4r_v^4F_{10}\right]-\frac{z_ir_v^2}{pR_m^3}\left[1+\frac{15r_i^2r_v^2}{8R_m^4}\right]$$
$$+\frac{3r_v^2X_m}{2R_m^5}\left[z_i\sin 2\alpha_{0m}+y_i\cos 2\alpha_{0m}\right] \tag{14}$$

where the algebraic term containing p^{-1} comes from $Xr_v\cos(\alpha_j+\theta_i)/R^{-3}$ in Eq. (4), which has no counterpart in Eq. (2). Again, the F_2 term was the only one given by Wood and Gordon.[12] Only the lowest order α term is included, as experience showed the others were not needed. The equation for $I_{vr}(2)$ is obtained from Eq. (14) simply by replacing z_i and y_i with y_i and $-z_i$, respectively, and so will not be given. There is, therefore, a considerable number of terms common to the three remainders, and this reduces the time required for their evaluation.

Discussion of Method 1

The expansion of Eq. (7) will be efficacious only when $2\delta \ll 1$, whereas 2δ can have any value between zero and unity, with the latter occurring when $r_i=r_v$ and $X=0$. Therefore, the computational efficiency, which should increase with N for the reasons given following Eq. (10), should also depend on r_i and r_v. Our numerical experiments showed the worst efficiency occurred typically when $r_v=2r_i/3$, $N=2$ and small p. For this reason, the parameters used for demonstration by Chiu and Peters[6]—$r_i=0.9$, $r_v=0.6$, $\theta_i=\theta_v=\pi/2$, $x_i=x_v$, $p=0.05$ and $N=2$—constitute a test of the present method that is close to the worst possible. We will discuss $I_{ur}(2)$ first. Figure 2 shows $I_u(2)$ and $I_{ur}(2)$ defined by Eq. (11) for these parameters. The dotted lines show the relationship between $I_u(2)$, $I_{ur}(2)$ and the bounding functions used to determine the remainders of Refs. 6, 10, and 11. Since the only nonzero α terms in the series expansion of $I_u(2)$ contain even powers of $\cos\alpha_0$, $I_u(2)=2r_v^2/R^3$ whenever $\cos\alpha_0=0$. Thus, $2r_v^2/R^3$ is always an exact bound on $I_u(2)$, but not always the upper bound shown in Fig. 2. Similarly, when $\cos\alpha_0=\pm 1$ or $\cos^2\alpha_0=1$, Eq. (11) approximates the other bound as shown in the figure. (The difference between this approximate bound and the minimum values of the dashed curve is due to the truncation of the α terms in Eq. (13), as described in the text preceding the equation.) Unfortunately, this neat relationship between $I_{ur}(2)$ and the bounds to $I_u(2)$ does not carry over to the other components or to $I_u(N)$ for $N>2$. $I_w(2)$ and $I_{wr}(2)$, defined by Eq. (14), are shown in Fig. 3.

Chiu and Peters[6] demonstrated the usefulness of their remainders by finding the value of θ_m that gave an absolute error ϵ of 10^{-4} for all three integrals. (In this paper, all errors are absolute errors.) For the test case defined earlier, θ_m varied between 15π and 20π, depending upon the component, whereas nearly 100 times these values were required for similar accuracy without using the remainders. Because it is simplest to calculate I_u, I_v, and I_w concurrently in an actual aerodynamic program, and θ_m would be an input parameter, the small variation in θ_m between components is highly desirable.

Similar calculations for the present remainders are summarized in Table 1. Each integral was evaluated first from $\theta=0$ to $\theta=\theta_0$ and then in steps of π; $\theta_0=\pi$ for the results in Table 1. The integral plus remainder was then compared to the "exact" value (including the remainder) after 400 steps. The results show the effects on θ_m of varying the order of both the F terms and α terms. With F_2 only, the values of θ_m for $I_u(2)$, 95π and $I_w(2)$, 59π are similar to those given by Wood and Gordon,[12] but the result for $I_v(2)$ is not. The reason is that no F term

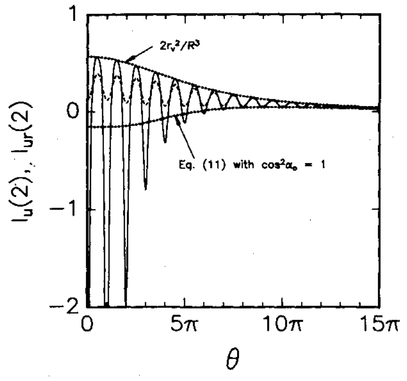

Fig. 2 $I_u(2)$ **(solid curve) and integrand for** $I_{ur}(2)$ **as defined by Eq. (13) (dashed curve):** $p = 0.05$, $x_i - x_v = 0$, $\theta_i = \theta_v = \pi/2$, $r_i = 0.9$, **and** $r_v = 0.6$; **dotted lines show bounds to** $I_u(2)$ **as explained in the text.**

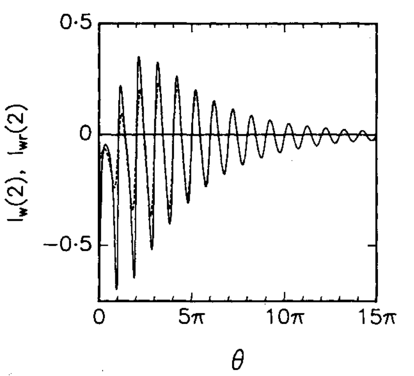

Fig. 3 $I_w(2)$ **(solid curve) and integrand for** $I_{wr}(2)$ **as defined by Eq. (14) (dashed curve):** $p = 0.05$, $x_i - x_v = 0$, $\theta_i = \theta_v = \pi/2$, $r_i = 0.9$, **and** $r_v = 0.6$.

contributes to $I_{vr}(2)$ when $z_i = 0$, as in the test case, so the remainder is dominated by the equivalent of the second bracketed term in Eq. (14). This term was not considered in Ref. 12, which resulted in a much larger θ_m. Increasing the order of the F terms generally reduces θ_m for $I_u(2)$, but increasing the order of the α terms has no effect, whereas nearly the opposite occurs for $I_w(2)$. The small difference between θ_m for F_6 and F_{10} suggests that there would be little point in further extending the order of the F terms. At face value, the effect of increasing the order of the α terms on $I_w(2)$ does suggest the importance of higher orders, but this was found not to be the case. The results in Table 1 indicate that the present remainders should give a computational efficiency similar to that achieved in Ref. 6. As p increases, the order of the F terms can be reduced while maintaining a very rapid convergence. As an example, with $p = 0.2$ but with the other parameters as above, θ_m for $I_u(2)$ was 6π for F_6, F_8, and F_{10}.

No use has yet been made of a unique feature of the present remainders—the retaining of some α dependence. The possibility of exploiting this feature was investigated using the test case (with $p = 0.05$) and choosing θ_0 to be a fraction of π. Some reductions in θ_m could be achieved, such as to 8.25π for $I_v(2)$. However, there seemed to be no clear pattern to the reductions, and the large ones seemed to be special cases, in the sense that the quoted reduction in θ_m for $I_w(2)$ did not occur when the same θ_0 was used for the other components. For the reasons given earlier, only a reduction in θ_m for all components is likely to be useful. Generally, the inclusion of the α terms did not have a large effect on θ_m, apart from making it less sensitive to the value of θ_0. This observation is supported by the behavior of the remainders for $N = 4$, which are obtained from Eqs. (13) and (14) by doubling the right side and removing the terms containing $\cos 2\alpha_{0m}$, as suggested by Eq. (10). This

Table 1 θ_m **for** $\epsilon < 10^{-4}$ **as a multiple of** π **for** $p = 0.05$, $r_i = 0.9$, $r_v = 0.6$, $\theta_i = \theta_v = \pi/2$, $N = 2$

Highest F term	$I_u(2)^a$	$I_u(2)^b$	$I_w(2)^a$	$I_w(2)^c$	$I_v(2)^a$	$I_v(2)^c$
None	___	___	___	___	18	18
F_2	95	95	59	45	___	___
F_4	34	34	53	24	___	___
F_6	23	23	53	18	___	___
F_8	13	13	53	17	___	___
F_{10}	17	17	53	17	___	___

[a]θ_m without α term. [b]θ_m with p^0, p^1 α terms. [c]θ_m with p^0 α term.

halves the period of I_u and I_w and reduces the effect of the α terms. Nevertheless, the values of θ_m were not significantly different from those given in Table 1.

It is possible that θ_m depends nonlinearly on the algebraic and α terms, as suggested by the minimum θ_m in Table 1 occurring for F_8 rather than F_{10}. Consider the following rough argument based on Fig. 2. The difference between the exact bound and the integrand of $I_{ur}(2)$ depends on the order of the algebraic terms, whereas it was mentioned previously that the difference between the approximate bound and the integrand depends on the order of the α terms. Thus, the two orders could be adjusted to "center" the integrand and so reduce θ_m. The efficacy in doing this is probably restricted to the axial velocity because the algebraic terms are usually not important for I_v and, generally, it is not possible to construct useful bounds for the integrands; recall that $I_u(2)$ is a special case in this regard.

It was noted in the previous section that the remainders with $\theta_m = 0$ can replace numerical integration when $r_i \ll r_v$ or $r_v \gg r_i$. A similar replacement is possible if the far-wake begins sufficiently far from the blades, that is, when $x_v - x_i$ is large.

Method 2: Euler-Maclaurin Summation

The infinite integral in Eq. (1) can be rewritten as a finite integral of an integrand containing the sum of an infinite series. Thus,

$$I_u(j,N) = r_v \int_0^{2\pi} [r_v - r_i \cos\alpha_j] \left[\sum_{k=0}^{\infty} f(\theta + 2\pi k) \right] d\theta \qquad (15)$$

where

$$f(\theta + 2\pi k) = R^{-3}(\theta + 2\pi k) = [R_\alpha^2 + (X + 2\pi pk)^2]^{-3/2}$$

$$R_\alpha^2 = r_i^2 + r_v^2 - 2r_i r_v \cos\alpha_j$$

and, for this section only, θ is limited to the range $0 \le \theta \le 2\pi$. Note that R_α is not defined as a function of j to emphasize that the summation must be performed separately for each vortex, and there is no further summation to zero as in Method 1. The sum (for each blade) can now be approximated using the Euler-Maclaurin formula:

$$\sum_{k=0}^{\infty} f(\theta' + 2\pi k) = \frac{1}{2\pi p} \int_{X'}^{\infty} f(s)\, ds + \frac{1}{2} f(\theta') - \frac{\pi p}{6} f'(\theta')$$

$$+ \frac{(\pi p)^3}{90} f'''(\theta') - \frac{(\pi p)^5}{945} f^{v}(\theta') + \cdots \qquad (16)$$

where X' is X at θ', s is a dummy variable, and all derivatives are with respect to X. The use of θ', rather than θ, indicates that Eq. (16) is not restricted to angles less than 2π. Equation (16) is valid only when $f(\theta' + 2\pi k)$ is infinitely differentiable, and $f(\theta' + 2\pi k)$ and all derivatives tend to zero as $k \to \infty$. (Note that infinite differentiability is a feature of any solution to Laplace's equation.) In addition, it is useful only when $f(s)$ can be integrated analytically. Fortunately, all of these conditions hold for f as defined by Eq. (15). Performing the integration gives

$$\sum_{k=0}^{\infty} R^{-3}(\theta'+2\pi k) = \frac{1}{2\pi p R_\alpha^2}\left[1-\frac{X'}{R(\theta')}\right] + \frac{R^{-3}(\theta')}{2} + \Sigma_R(\theta') \tag{17}$$

where

$$\Sigma_R(\theta') = \frac{\pi p X'}{R^5(\theta')}\left\{\frac{1}{2}+\frac{(\pi p)^2}{2R^2(\theta')}\left[1-\frac{7X'^2}{3R^2(\theta')}\right] + \frac{(\pi p)^4}{R^4(\theta')}\left[\frac{5}{3}-\frac{10X'^2}{R^2(\theta')}+\frac{11X'^4}{R^4(\theta')}\right]\right\}+\cdots$$

and $R(\theta')$ is R at θ'. Note that $\Sigma_R(\theta')$ is a sum in odd powers of p and so only a few terms should be needed. Only those terms shown explicitly in Eq. (17) were considered in this study. The distinction between θ and θ' can now be exploited; for any θ, the series can be summed exactly up to $\theta' = \theta + 2\pi m$, where m is an integer, and the remaining sum can be approximated by Eq. (17). For the integrand of Eq. (15), this gives

$$\sum_{k=0}^{\infty} R^{-3}(\theta+2\pi k) \approx \sum_{k=0}^{m} R^{-3}(\theta+2\pi k) + \text{RHS of Eq. (17)} \quad \text{for } \theta' = \theta + 2\pi m \tag{18}$$

Equation (18) is similar in form to Eq. (5), which is the basis of Method 1. However, neither of the terms in Eq. (18) leads to analytical integrals, and so the final component of Method 2 is a numerical integration.

To calculate the other induced velocities, an additional sum

$$\sum_{k=0}^{\infty} f(\theta+2\pi k) \quad \text{where} \quad f = (X+2\pi k)R^{-3}(\theta+2\pi k)$$

is required. Fortunately, it is amenable to the same techniques, so that Eq. (16) gives

$$\sum_{k=0}^{\infty}(X+2\pi pk)R^{-3}(\theta'+2\pi k) = \frac{1}{2\pi p R(\theta')} + \frac{1}{2}\left(X'-\frac{\pi p}{3}\right)R^{-3}(\theta') + X'\Sigma_R(\theta') - \frac{(\pi p)^3}{R^5(\theta')}\left\{\frac{1}{10}-\frac{X'^2}{2R^2(\theta')}+\frac{5(\pi p)^2}{R^2(\theta')} \times \left[\frac{1}{21}-\frac{2X'^2}{3R^2(\theta')}+\frac{X'^4}{R^4(\theta')}\right]\right\}+\cdots \tag{19}$$

which is analogous to Eq. (17). Again, only the terms shown explicitly were used, the resulting integral has to be evaluated numerically, and there is no summing to zero when $N \geq 2$, so each vortex must be treated separately. This is the second main difference from Method 1. The third difference is that Method 2 does not have separate algebraic and α terms.

General Discussion

The observations at the end of the last section suggest that Method 2 will, in general, be less efficient than Method 1. Nevertheless, it does offer certain advantages. Our numerical experiments showed that the method gave accurate results for all three components with $m = 1$ over the range $0.05 \leq p \leq 0.5$, with the other parameters as before. Some fine tuning would probably reduce the order at high p, but we did not pursue this because Method 2 is more appropriate at small pitch, for the reasons contained in Fig. 4, where the integrand is plotted from Eq. (18) for $p = 0.05$ and 0.5. It is obvious, as it is from the plots for the other velocities not shown, that the integrands tend toward periodicity as p decreases. Periodicity suggests the use of the trapezoidal rule, which is simple and easily implemented with interval halving to achieve a specified accuracy. Furthermore, the accuracy is specified over one interval only. Of course, the integration in Method 1 could be done over only one interval, but this would require prior knowledge of θ_m. Both the trapezoidal and Gauss-Legendre rule have been used with Method 2; the latter is better suited to higher values of the vortex pitch.

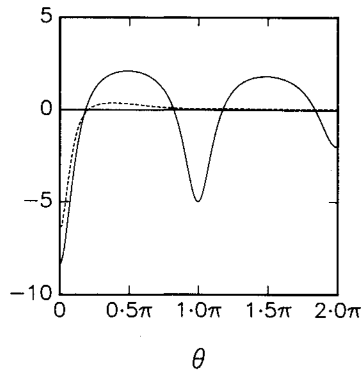

Fig. 4 Integrand for $I_u(2)$ from Method 2: $x_i - x_v = 0$, $\theta_i = \theta_v = \pi/2$, $r_i = 0.9$, and $r_v = 0.6$; solid curve for $p = 0.05$, dashed curve for $p = 0.5$.

Method 2 is the more general and robust and appears particularly useful as a test for other methods. As an example, the results in Table 1 were obtained using Romberg integration, with an error per step that was hopefully small enough to give an overall error of less than 10^{-6} using double precision. This gave $I_u(2) = -2.0\times10^{-4}$, whereas Method 2 gave -1.9×10^{-4}, which agrees with the value given by Chiu and Peters.[6] The difference here is due to the accumulation of round-off errors in the Romberg method. Although the difference, about 10^{-15}, is too small to affect the results in Table 1, it does serve as a warning of possible numerical problems.

We have not attempted a detailed comparison of our remainders with those of Ref. 6 because the comparison will depend partly on factors other than the form of the remainders, such as the integration method. Instead, copies of all of the programs used here for $N = 2$ can be obtained without cost from the first author.

Summary and Conclusions

This paper describes two methods for numerically evaluating the infinite integrals for the velocities induced by constant diameter helical vortices. These occur in the far-wakes of wind turbines, propellers, and, in some cases, helicopter rotors. Both methods use an analytic approximation to avoid the infinite range of integration. In the first method, the integrand for each vortex is expanded as a series, and the integrands of all vortices of the same radius are summed prior to integration. This reverses the order used in deriving the remainders of Refs. 6, 10, and 11, and has the advantage of canceling many terms. The terms that do not cancel are either ignored or integrated to give the analytic remainders of Eqs. (13) and (14). At small values of vortex pitch the computational efficiency is similar to that achieved by remainders formed from bounding functions (Refs. 6, 10, and 11). As the pitch increases to values typical of propellers and wind turbines, Eqs. (13) and (14) can be simplified while maintaining rapid convergence. In certain circumstances, such as when the far-wake begins sufficiently far from the blades, the remainders can totally replace numerical integration.

Method 2 is based on recasting the infinite integral as a finite one whose integrand contains one or two infinite series. Each series is summed exactly up to some limit, and the remaining sum is approximated using the Euler-Maclaurin formula. Numerical integration is always needed, and the method is more cumbersome in that each vortex must be considered separately; there is no summation to zero, as in Method 1. However, the implementation of Method 2 is less sensitive to changes in vortex pitch and to the angle dependence of all of the integrals, so it can be relied upon to give accurate results over a wide range of parameters. As p decreases, the integrands tend toward periodicity and can then be integrated quickly and accurately using the trapezoidal rule.

Acknowledgments

This work was supported by the Australian Research Council. Some very useful comments made by one of the reviewers have been incorporated into this paper.

References

[1]Langrebe, A. J., "The Wake Geometry of a Hovering Helicopter Rotor and Its Influence on Rotor Performance," *Journal of the American Helicopter Society,* Vol. 17, Oct. 1972, pp. 3-15.

[2]Kerwin, J. E., "Marine Propellers," *Annual Review of Fluid Mechanics,* Vol. 18, 1986, pp. 367-403.

[3]Hess, J. L., and Valerazo, W. O., "Calculation of Steady Flow Around Propellers Using a Surface Panel Method," *Journal of Propulsion and Power,* Vol. 1, Nov.-Dec. 1985, pp. 470-476.

[4]Valerazo, W. O., and Liebeck, R. H., "Three-Dimensional Calculation of Windmill Surface Pressures," AIAA Paper 88-2533, June 1988.

[5]Afjeh, A. A., and Keith, T. G., "A Simplified Free Wake Method For Horizontal-Axis Wind Turbine Performance Prediction," *Journal of Fluids Engineering,* Vol. 108, Dec. 1986, pp. 400-406.

[6]Chiu, Y. D., and Peters, D. A., "Numerical Solutions of Induced Velocities by Semi-infinite Tip Vortex Lines," *Journal of Aircraft,* Vol. 25, Aug. 1988, pp. 684-694.

[7]Hess, J. L., and Smith, A. M. O., "Calculation of Potential Flow about Arbitrary Bodies," *Progress in the Aerospace Sciences,* Vol. 8, 1966, pp. 1-138.

[8]Hess, J. L., "The Problem of Three-Dimensional Lifting Potential Flow and Its Solution by Means of Surface Singularity Distribution," *Computer Methods in Applied Mechanics and Engineering,* Vol. 4, July 1974, pp. 283-319.

[9]Miller, R. H., "The Aerodynamics and Dynamic Analysis of Horizontal Axis Wind Turbines," *Journal of Wind Engineering and Industrial Aerodynamics,* Vol. 15, Nov. 1983, pp. 329-340.

[10]Rand, O., and Rosen, A., "Efficient Method of Calculating the Axial Velocities Induced Along Rotating Blades by Trailing Helical Vorticity," *Journal of Aircraft,* Vol. 21, No. 6, 1984, pp. 433-435.

[11]Graber, A., and Rosen, A., "Velocities Induced by Semi-infinite Helical Vortex Filaments," *Journal of Aircraft,* Vol. 24, No. 5, 1987, pp. 289, 290.

[12]Wood, D. H., and Gordon, G., "On the Evaluation of the Velocities Induced by Trailing Helical Vortices," *AIAA Journal,* Vol. 28, No. 4, 1990, pp. 754-756.

[13]Andersen, S. V., and Andersen, P., "Hydrodynamic Design of Propellers with Unconventional Geometry," *Transactions Royal Institute of Naval Architects,* Vol. 128, May 1986, pp. 201-221.

[14]Gradshteyn, I. S., and Rhysik, I. M., *Tables of Integrals, Series and Products,* edited by A. Jeffries, Academic Press, New York, 1980.